Proteomics and gene expression analyses of mitochondria from squalene-treated apoE-deficient mice identify short-chain specific acyl-CoA dehydrogenase changes associated with fatty liver amelioration

Adela Ramírez-Torres[1], Silvia Barceló-Batllori[2], Erika Fernández-Vizarra[3], María A. Navarro[3], Carmen Arnal[4, 5], Natalia Guillén [1,5], Sergio Acín[3], Jesús Osada[1, 5]

[1] Departamento Bioquímica y Biología Molecular y Celular, Facultad de Veterinaria, Instituto de Investigación Sanitaria de Aragón (IIS), Universidad de Zaragoza, Spain

[2] Unidad de Proteómica, IIS Aragón. Zaragoza, Spain

[3]Unidad de Investigación Traslacional. IIS Aragón. Hospital Universitario Miguel Servet. Zaragoza, Spain

[4] Departamento de Patología Animal, Facultad de Veterinaria, Universidad de Zaragoza, Spain

[5] CIBER de Fisiopatología de la Obesidad y Nutrición, Instituto de Salud Carlos III, Spain

Correspondence to: Jesús Osada, PhD,
Department of Biochemistry and Molecular Biology,
Veterinary School, University of Zaragoza,
Miguel Servet, 177, E-50013 Zaragoza, Spain.
Fax number: 34-976-761612
Telephone number: 34-976-761644
E-mail: josada@unizar.es

Abstract

Squalene, a hydrocarbon involved in cholesterol biosynthesis, is an abundant component in virgin olive oil. Previous studies showed that its administration decreased atherosclerosis and steatosis in male apoE-knock-out mice. To study the effect of squalene on mitochondrial proteins in fatty liver, 1 g/kg/day of this isoprenoid was administered to those mice. After 10 weeks, hepatic fat was assessed and protein extracts from mitochondria enriched fractions from control and squalene-treated animals were analyzed by 2D-DIGE. Spots exhibiting significant differences were identified by MS/MS analysis. Squalene administration modified the expression of eighteen proteins involved in different metabolic processes, 12 associated with hepatic fat content. Methionine adenosyltransferase I alpha (*Mat1a*) and short-chain specific acyl-CoA dehydrogenase (*Acads*) showed significant increased and decreased transcripts, respectively, consistent with their protein changes. These mRNAs were also studied in wild-type mice receiving squalene, where *Mat1a* was found increased and *Acads* decreased. However, this mRNA was significantly increased in the absence of apolipoprotein E. These results suggest that squalene action may be executed through a complex regulation of mitochondrial protein expression, including changes in *Mat1a* and *Acads* levels. Indeed, *Mat1a* is a target of squalene administration while *Acads* reflects the anti-steatotic properties of squalene.

Keywords: fatty liver, squalene, proteomics, mitochondria, *Acads*, *Mat1a*

Introduction

Non-alcoholic fatty liver (NAFLD) or hepatic steatosis has become the most common chronic liver disease in adults and children in Western societies. Most patients develop simple hepatic steatosis with only a few of them developing a spectrum of liver injuries ranging from steatosis to progressive steatohepatitis, cirrhosis and hepatocellular carcinoma [1, 2]. Excessive energy intake in these societies greatly contributes to the development of NAFLD paralleling its prevalence to that of the epidemics of obesity [3]. Inappropriate dietary fat intake, insulin resistance and increased oxidative stress can result in increased hepatic triglyceride accumulation and originate steatosis, in two different presentations: microvesicular and macrovesicular steatosis, although both forms may coexist. Microvesicular steatosis is characterized by small and multiple lipid droplets surrounding a centrally placed nucleus whereas in macrovesicular steatosis, hepatocyte is distended by a single vacuole displacing the nucleus to the periphery of the cell. Steatosis is associated with a more long-standing disturbance of hepatic lipid metabolism and with the development of more advanced complications: steatohepatitis, fibrosis and cirrhosis [4]. Hepatic steatosis is an entity not only compromising lipid metabolism [5], inducing also whole genome expression changes [6] demanding high-throughput approaches for its study. Therefore, given the relevance of the initial steatosis, it is critical to get ot know its mechanisms to find potential therapies in early stages of the disease.

Olive oil, as a main source of fat in the Mediterranean diet, has shown to ameliorate fatty liver by decreasing hepatic triglyceride accumulation and postprandial response [7], an effect mainly attributed to its monounsaturated fatty acid content [8]. However, administration of different virgin olive oils showed changes at the proteomic level and in the degree of hepatic steatosis that were not directly related to the oleic acid content

71 [9]. In fact, olive oil is a functional food that contains saponifiable and unsaponifiable
72 fractions, the latter also named minor components [10]. Evidence for the benefits of
73 these minor components has been documented [11-13]. Squalene is the major
74 component of the unsaponifiable fraction and its content in virgin olive oil is greatly
75 variable, from 1.5 to 9.6 g/ kg [14]. Likewise, the average intake of squalene ranges
76 from 30 mg/day in the United States up to 400 in Mediterranean countries [15].
77 Furthermore, Gylling and Miettinen documented consumes of up to 1g of squalene per
78 day in some diets [16]. Due to this high biological tolerance, it has been successfully
79 used to treat alcohol damage in the chick embryo retina [17]. Our group showed that a
80 high squalene dose decreased hepatic fat content in a sex-dependent manner [18] in
81 apoE-deficient mice, a well-characterized and widely used animal model which rapidly
82 develops atherosclerotic lesions similar to those observed in humans [19]. ApoE
83 deficiency in these animals leads to a moderate or severe hepatic steatosis when fed
84 standard chow or a high fat diet, respectively [20]. The hepatic fat content has been
85 associated with the development of atherosclerotic lesions [21] and modulated by
86 dietary interventions [7, 22].

87 Mounting evidence suggests that mitochondrial dysfunction and more specifically
88 respiratory chain deficiency plays a key role in non-alcoholic steatohepatitis by
89 impairing not only fat homeostasis in the liver but also leading to overproduction of
90 reactive oxygen species (ROS) that trigger lipid peroxidation, cytokine overproduction
91 and cell death [23]. Mitochondria are essential organelles that accomplish several vital
92 functions including ATP production through oxidative phosphorylation, signal
93 integration, apoptosis and cellular senescence, dissipation of heat, anabolic processes,
94 calcium homeostasis and fatty acid metabolism. The involvement of both apolipoprotein
95 E and mitochondria in lipid metabolism is widely recognized [24, 25], however, there

96 are surprisingly scarce data concerning the involvement of this protein in mitochondrial
97 metabolism [26]. Since mitochondria play a central role in cellular lipid catabolism, and
98 squalene decreases hepatic fat content, our working hypothesis was that squalene
99 administration could modify hepatic mitochondrial proteins linked to hepatic steatosis.
100 To address such issues and gain more insight into the mechanisms involved in the
101 action of dietary squalene supplementation on the mitochondrial proteome, 2D-
102 fluorescence DIGE analysis was used to study the modifications caused by squalene in
103 apoE-ko mice. Firstly, mitochondrial fractions were obtained by differential
104 centrifugation. Secondly, proteomic experiments were performed to separate proteins.
105 Using gel image analysis, differences in protein expression between both experimental
106 conditions were searched. Those proteins displaying significant differences (higher than
107 1.18 fold change) were identified by mass spectrometry and considered putative
108 squalene targets. Thirdly, their expression changes were also analyzed at the mRNA
109 level. Finally, the candidate genes were also analyzed in squalene-fed wild-type mice to
110 distinguish the solely squalene administration effects in these animals, from those
111 related to fatty liver present in the apoE-ko mice which were modified by administrating
112 this compound.

113

2. Methods and materials

2.1 Animal experiments

Male homozygous apoE-ko mice, hybrids of C57BL/6J×129 Ola strains aged 2 months were bred at *The Unidad Mixta de Investigación* (University of Zaragoza). Two different groups were established: squalene group (n=5) whose beverage contained 1% (v/v) of squalene in glycerol solution and control group (n=5) which received glycerol solution used as vehicle. The squalene dose was 1 g/kg/day for 10 weeks as previously described [18]. Both groups were daily fed with mice chow, Teklad Mouse/Rat Diet no. 2014 (Harlan Ibérica, Barcelona Spain). In the same way, two groups of C57BL/6J background wild-type mice were established: control (n=6) and squalene (n=7). The same protocol was applied to the wild-type mice and was well tolerated, as there was no incidence on survival, physical appearance and solid and liquid intakes. After the experimental period, animals were sacrificed by suffocation in CO_2 and livers were removed and frozen in liquid nitrogen. The protocol was approved by the Ethical Committee for Animal Research of the University of Zaragoza.

2. 2. Liver histology of apoE-deficient mice

Liver tissue samples were stored in neutral formaldehyde and included in paraffin. Sections (4 μm) were stained with hematoxylin and eosin. Hepatic fat content was evaluated by quantifying the extent of fat droplets in each liver section with Adobe Photoshop 7.0 and expressed as the percentage of total liver section. The diameter of 100 fat droplets of each mouse was also measured by means of Scion Image software (Scion Corporation, Frederick, Maryland, USA).

2.3. Subcellular fractionation

For the preparation of mitochondria in apoE-ko and wild-type mice, livers were homogenized in PBS (4 ml/g of tissue) with protease inhibitor cocktail tablets (Roche)

using a Potter homogenizer. Debris tissue was removed by centrifugation at 200 x g for 10 min at 4ºC. The homogenate was spun down at 1000 x g for 15 min. The supernatant containing mitochondria was centrifuged at full speed, 13000 x g for 2 min. The mitochondrial pellets were washed twice, pelleted, resuspended in PBS and spun for 1 min [27]. Mitochondrial protein was quantified by Bradford assay.

2.4. Mitochondrial content and functionality assays

Liver mitochondria for functional assays, from squalene-fed or untreated mice, were isolated as described [28]. Respiratory activity, i.e. oxygen consumption, in freshly isolated liver mitochondria was measured by high-resolution respirometry with the Oxygraph 2K instrument in wild-type mice (Oroboros Instruments, Insbruck, Austria). Briefly, 140-160 micrograms of mitochondrial protein were added to 2 ml of MAITE medium (25 mM sucrose, 75 mM sorbitol, 100 mM KCl, 0.05 mM EDTA, 5 mM MgCl2, 10 mM Tris and 10 mM phosphate, pH 7.4) in the presence of 1 mg/ml fatty acid-free BSA, 10 mM glutamate and 2.5 mM malate. State 3 respiration was induced by addition of 1 mM ADP. Oxygen consumption was completely inhibited when 2 mM KCN was added to the chamber. Kinetic assays for the determination of cytochrome c oxidase (COX) and citrate synthase (CS) activities in the same mitochondrial fractions were measured spectrophotometrically [29]. Subsequently, the same liver mitochondria were solubilised with 1.6 mg dodecylmaltoside (DDM) per mg mitochondrial protein to be run through blue-native gel electrophoresis (BNGE) [30]. Complex I in-gel activity assay was performed after BNGE as described [31]. Western blot was also performed after native electrophoresis and the mitochondrial respiratory chain complexes were immunodetected using antibodies against specific subunits (Mitosciences).

2.5. Sample preparation for DIGE analysis

Samples from apoE-ko mice were prepared as previously described [32]. Briefly, proteins were precipitated using the 2D clean-up kit (GE Healthcare) and resuspended in a buffer containing 30 mM Tris, 7 M urea, 2 M thiourea, 4% CHAPS, pH was adjusted to 8.5, and finally protein content was quantified using the RC/DC Protein Assay (Bio-Rad Laboratories).

2.6. Two-dimensional electrophoresis

Five biological replicates of each experimental condition of apoE-deficient mice were analyzed by 2D-DIGE. Mitochondrial protein samples were minimally labeled with Cy3 and Cy5 fluorescent dyes (25 μg of protein/200 pmol of dye) as previously described [32]. An internal standard was prepared mixing equal amount of mitochondrial proteins from control and squalene groups with Cy2. IPG strips (pH 3–10, 24 cm, GE Healthcare) were rehydratated using 450 μl of Destreak solution (GE) with IPG buffer (0.05% v/v) overnight. The IPG strips were cup-loaded with 25 μg of each Cy2-, Cy3- and Cy5-labeled sample in a buffer containing 7 M urea, 2 M thiourea, 2% (w/v) CHAPS, 65 mM DTT, and 1% (v/v) IPG buffer. Isoelectric focusing was carried out in a Protean IEF cell (Bio-Rad) at 62 kV-h in different phases as follows: 10 min at 50 V, 1-h ramp up to 500 V, 1 h at 500 V, 2-h ramp up to 1000 V, 10-h ramp up to 10,000 V, and 2-h at 10,000 V. Prior to second dimension SDS-PAGE, the strips were equilibrated for 15 min in DTT buffer (375 mM Tris-HCl pH 8.8, 6 M urea, 20% v/v glycerol, 2% w/w SDS and 130 mM DTT), followed by another 15 min incubation in iodoacetamide (375 mM Tris-HCl pH 8.8, 6 M urea, 20% v/v glycerol, 2% w/w SDS and 135 mM iodoacetamide). SDS-PAGE was run by overlaying the strips on 10% isocratic Laemmli gels (24 x 20 cm), overnight at 20ºC on a Protean Plus Dodeca Cell (BioRad) at 1 W/gel until the bromophenol blue tracking front reaches the end of the gel. For protein identification, a preparative gel including 300 μg of mitochondrial protein (50 μg Cy2

189 labeled) was also performed and cy2 image obtained (see section 2.7). The preparative
190 gel was fixed with 50% ethanol/10% acetic acid, 2 times for 20 min each, and washed 3
191 times, 10 min each with water. The gel was stained using a fresh solution of Colloidal
192 Coomassie. Firstly, it was shaked for 1 hour in an aqueous solution containing 16%
193 ammonium sulphate, 3 % (v/v) phosporic acid and 32 % (v/v) methanol. Then, it was
194 transferred to a 6.6% Coomassie Blue G-250 methanolic solution for 3 days. Destaining
195 was carried out by immersing the gel in water with frequent changes.

196 **2.7. Gel scanning and image analysis**

197 Fluorescence images of the gels were acquired on a Typhoon Trio 9000 scanner (GE
198 Healthcare). Gels were scanned individually and the Photo Multiplier Tube voltage was
199 adjusted for maximum image quality with minimal signal saturation. Images were
200 checked for saturation during the acquisition process using ImageQuant TM TL
201 Software (GE Healthcare). Cy2, Cy3, and Cy5 images for each gel were scanned at
202 488/510-, 532/530-, and 633/500-nm excitation/emission wavelengths, respectively, at
203 100-μm resolution, thus obtaining a total of 15 images (5x3).

204 Determination of protein spot abundance was performed using the Progenesis
205 SameSpots v4.0 software (Nonlinear Dynamics, U.K.). Statistically significant changes
206 in protein spots were determined using ANOVA test ($P < 0.05$) and a cut-off of 1.18 fold
207 change was established for further analyses. The protein spots from analytical gels were
208 matched to the corresponding Cy2 and Coomassie preparative gel image. Protein spots
209 were manually picked from the Coomassie blue–stained gel.

210 **2.8. In-gel digestion**

211 Protein spots were excised manually from preparative 2D gel and processed as
212 previously described with minor modifications [32]. Briefly, spots were washed with
213 water, ammonium bicarbonate (25 mM) and acetonitrile. Next, samples were reduced

and alkylated by incubation with DTT (10mM) at 60 °C during 45 min followed by incubation with iodoacetamide (50 mM) at room temperature during 30 minutes. Finally, proteins were digested with trypsin overnight at 37ºC (2.5–1.25 ng/µl, ratio enzyme: protein 1:20, Trypsin Gold, Mass Spectrometry Grade, Promega). Digestion was stopped by addition of 0.5% TFA, and tryptic peptides were extracted in two steps by incubating the gel pieces with 0.1% TFA/H_2O and 60% ACN for at least 30 min. A final extraction was performed using 100% ACN. All extracts were then combined, and peptides were concentrated and passed through ZipTip C18 tips (Millipore) to remove salt and detergent traces following the manufacturer's instructions.

2.9. Mass spectrometry analyses

Sample and matrix, a saturated solution of alpha-cyano-4-hydroxycinnamic acid in 50% ACN/0.1% TFA/H_2O, were spotted in duplicate onto an Opti-Tof 384 well insert plate (Applied Biosystems). MALDI-TOF MS was performed using a 4800plus MALDI-TOFTOF (Applied Biosystems) in the reflector mode with accelerating voltage of 20 kV, mass range of 800 to 4000 Da and 1000 shots/spectrum. MS/MS spectra were acquired automatically on the 20 most intense precursors and calibrated using a standard protein mixture (4700 Calmix, Applied Biosystems).

2.10. Protein identification and data-mining

Proteins were identified using the search engine Mascot (Matrix Science Ltd.) with the SwissProt database 57.15. Search parameters were set as follows: mammalian taxonomy (64838 sequences), missed cleavage 1, fixed modifications carbamidomethyl (cysteines) and peptide tolerance 0.1 Da and fragment mass tolerance 0.3 Da. Proteins with a score above 61($P<0.05$) were considered as a positive hit. The Protein Analysis

Through Evolutionary Relationships (PANTHER) resource was used to classify data into different categories (www.pantherdb.org).

2.11. RNA isolation and quantitative PCR analyses

RNA from 100-mg liver of apoE-ko and wild-type mice was extracted using TriReagent (Sigma). DNA contaminants were eliminated using the DNA removal kit from AMBION (Austin, TX, USA). First-strand cDNA synthesis (5 μg) and PCR reactions were performed using the SuperScript II Platinum Two-Step RT-qPCR Kit with SYBR Green (Invitrogen, Madrid, Spain) as previously described [18]. The mRNA expression was analyzed by quantitative real time PCR (qPCR) of individual samples using equal amounts of RNA. The primers (Supplementary Table 1*)* according to MIQE guidelines [33] were designed using Primer Express software (Applied Biosystems, Foster City, CA). The relative quantification of gene expression was analyzed by the $2^{-\Delta\Delta Cq}$ method [34]. The mRNA expression corresponding to the *cyclophilin B* was used as the reference control.

2.12. Statistical analysis

Gene expression of the proteins determined by 2D-DIGE technique was analyzed using SPSS version 15.0 software (SPSS®, Chicago, IL). The Kolmogorov and Smirnov's test was used to verify whether the variables were normally distributed and the Levenne *F*-test to assess the homogeneity of variances. Since most variables did not exhibit a Gaussian distribution or failed to show homology of variances and due to the low sample size, comparisons were carried out using Mann–Whitney *U*-test. Correlation analyses were performed considering the relationship among individual normalised protein spot volume and 1) hepatic fat, 2) average droplet size of each mice. Also a correlation study between mRNA levels and hepatic fat was carried out. Spearman's test was used for the analysis. Significance was set at $P < 0.05$.

3. Results

3.1. Histological analyses

In one of our group's previous study, apoE-ko mice receiving squalene showed significant decrease in hepatic fat content compared to mice fed a control diet (control group 11.3 ± 6.1; squalene group 5.8 ± 3.5**)**. However, this agent did not modify plasma cholesterol, triglycerides and APOA5 levels [18]. In order to determine the droplet size distribution between both diet groups in apoE-ko mice, a total of 100 lipid droplets of each individual of the study were measured. Lipid droplet size significantly decreased in squalene-supplemented mice (control group 2.16 ± 0.02, squalene group 2.08 ± 0.03**;** Fig.1A). In addition, the latter group showed a significant minor frequency of 2-3 μm droplets ($P<0.05$) as reflected on the lipid droplet profile (Fig. 1B).

3.2. Mitochondrial content and functionality assays

Yield and functionality of the organelles of wild-type mice were tested by enzymatic assays, mitochondrial oxygen consumption and Blue Native. In each purification step, the specific activity of the mitochondrial marker enzyme succinate dehydrogenase was increased: initial homogenate had 8.0 ± 0.4 and the final mitochondria fraction had a specific activity of 27.3 ± 1.7 units/min/mg, indicating an enrichment of over 4-fold and a yield of mitochondria of over 9%.

State 3 respiration, an index of the ADP-stimulated oxygen consumption rate, was the same in isolated mitochondria in the two types of tested samples: pooled livers extracted from squalene-fed and non-squalene treated animals (data not shown). However, cytochrome c oxidase (COX or CIV) activity, normalized by the citrate synthase (CS) activity, was found to be significantly ($P<0.05$) increased in the squalene-treated mice (Fig. 2A). The increase in activity was not accompanied by elevated assembled COX

levels, as for the other respiratory chain complexes tested by BNGE and Western Blot (Fig. 2B). CI in-gel activity was apparently the same in all tested samples.

3.3. Hepatic proteomic profile after the supplementation of squalene in diet in apoE-ko mice

Separation and identification of mitochondrial hepatic proteins differentially regulated by squalene supplementation were carried out by 2D-DIGE. SameSpots software revealed statistically significant differences in 19 protein spots using ANOVA ($p<0.05$). Subsequently, after running a preparative Coomassie-stained gel, including cy2-labeled proteins, the selected spots were excised and identified by MALDI-MS, being the hits searched in the databases (Figure 3). This allowed correct spot matching between analytical and preparative gels, minimizing uncertainty and reducing the possibility of favouring unspecific cellular stress proteins to the detriment of the less abundant yet more meaningful ones. Fifteen protein spots showed at least -1.18-fold decreased expression in the squalene group compared to the control group, while 3 protein spots were increased (Table 1 and Supplementary Table 2). PANTHER [35] analysis using protein accession numbers resulted in two protein classifications according to their 1) biological processes and 2) molecular functions. Attending to the biological process criteria, the PANTHER gene ontology database grouped the proteins in 5 categories (Fig. 4A), the majority of which were implicated in metabolism (65%). Of these, 75% implicated in primary metabolic processes, that is, carbohydrate (30%), amino acid (30%), nucleic acid (20%) and protein and lipid (20%) metabolism (Fig. 4A). Attending to their molecular functions (Fig. 4B), the 90% of the differentially expressed proteins were involved in catalytic activity while 10% were transporters. Proteins with catalytic activity were oxidoreductases (35%), transferases (30%), hydrolases (9%) and isomerases, ligases, lyases (9% each, respectively).

3.4. Association between protein expression and fat accumulation

A correlation study was carried out to establish whether differences in protein expression (% normalized volume) induced by squalene intake might be associated with changes in hepatocyte fat accumulation. As reflected in Table 2, an inverse and statistically significant correlation was found among hepatic fat content and argininosuccinate synthase (ASSY), 3-ketoacyl-CoA thiolase (THIM) and S-adenosylmethionine synthase isoform type1 (METK1) levels. On the other hand, a direct and statistically significant association was found among hepatic fat and fumarylacetoacetase (FAAA), alpha-aminoadipic semialdehyde dehydrogenase (AL7A1), indolethylamine N-methyltransferase (INMT), short-chain specific acyl-CoA (ACADS) and sorbitol dehydrogenase (DHSO), adenylate kinase 2 (KAD2), carbonic anhydrase 3 (CAH3) and glutamate dehydrogenase (DHE3) contents.
Additionally, a direct association between alpha-aminoadipic semialdehyde dehydrogenase (ALDH2) protein content and diameter of lipid droplets was observed.

3.5. RNA analysis of differentially expressed proteins with qPCR

In order to support the observed squalene-induced protein changes, mRNA expression analyses of the 18 identified corresponding gene products were carried out in apoE-ko mice (Supplementary Table 3). *Mat1a* and *Acads* mRNA levels displayed significant changes after squalene supplementation (Fig. 5A). Their changes paralleled the findings in the proteomics analysis where METK1 (MAT1A) was augmented and ACADS was diminished in the squalene group. Statistical significant associations were also observed for changes in these mRNAs and hepatic fat content (Fig. 5B).

The fact that many protein changes were not observed at the mRNA level was not surprising. Protein and mRNA expression levels do not always show a direct

correlation, since protein turnover rate, stability, degradation, processing and posttranslational modifications are not reflected at the mRNA level [36]. There was no evidence of posttranslational modifications in the identified proteins because of the lack of deviations from the experimental pI and Mr, estimated by spot migration in the 2D gels, and their corresponding theoretical values. Further work will be required to identify the post-transcriptional mechanisms underlying the observed changes at the protein level and not in mRNA abundance.

To corroborate the induced *Mat1a* and *Acads* changes in a different model, wild-type animals were fed squalene, which allowed also to test its effects when the apolipoprotein E is present. In this experimental setting, independent of the effect of the lack of apoE (Fig. 5A), *Mat1a* mRNA expression was increased also, and to the same extent as in the previous model. On the other hand, we found that absence of apoE induced a significant increase of the *Acads* mRNA compared to wild-type animals. However, squalene consumption leads to a significant decrease of *Acads* gene expression in both animal models, being more pronounced in apoE-deficient mice, where the expression of this gene is originally higher. Collectively, these results are suggesting that induction of *Mat1a* and reduction of *Acads* levels are a response to squalene administration in both models.

3.6 Effect of squalene on mRNA expression of genes involved in lipid metabolism

In view of the results described previously, we decided to test the mRNA levels for other related factors necessary for lipid metabolism. As shown in Table 3, apoE-ko mice receiving squalene had significantly increased *Scd1, Cpt1a, Ppara, Ppargc1a* and *Cyp7a1* mRNA levels. The changes observed for *Cyp7a, Ppargc1a* and *Scd1* were significant and inversely correlated with hepatic fat content (Fig. 6). In wild-type mice, the expressions of *Acaca, Acab, Scd1, Ppara, and Cyp7a1* were increased in those

receiving squalene, while that of *Ppargc1a* was decreased. These results indicate that three genes *(Scd1, Ppara, and Cyp7a1*) involved in fatty acid and cholesterol catabolism are induced by squalene administration independently of apoE deficiency. On the other hand, *Acaca, Acab* and *Ppargc1a* responses to squalene were dependent on the phenotype induced by the absence of apoE.

4. Discussion

In this study, we have investigated the effect of the ingestion of 1 g/kg/day squalene, the major compound of the unsaponifiable fraction in virgin olive oil, on the development of hepatic steatosis and the underlying molecular mechanisms. For this purpose, we have analyzed and compared the liver mitochondrial proteome in apoE-ko mice ingesting a squalene-rich diet and their corresponding controls fed only with standard chow. Using 2D-fluorescence DIGE gels and image processing, eighteen proteins displaying significant differences, higher than 1.18-fold, were identified by mass spectrometry and considered putative squalene targets. Twelve of them had values associated with the fat content degree in the liver. Only two, *Mat1a* and *Acads* also showed significant changes at the mRNA levels, finding also a correlation between them and hepatic steatosis. When these candidate genes were analyzed in squalene-fed wild-type animals, their expression was modified in the same direction as in the ko animals. *Mat1a* expression was increased and *Acads* showed a decrease. Although for the latter gene, the absence of apolipoprotein E induced a significant increase in its mRNA levels. In addition, three genes *(Scd1, Ppara, and Cyp7a1*) involved in fatty acid and cholesterol catabolism were up-regulated by squalene administration whether apoE was present or not. Using both types of animals has allowed us to discriminate the effects of squalene administration with or without fatty liver and to delineate squalene-sensitive gene expression changes.

The proteomics methodology, and in particular two-dimensional electrophoresis, allows identification and quantification of large numbers of proteins in complex protein mixtures [37]. Intrinsic limitations of the 2DE/MS approach that can impede accurate quantitation and identification have to be considered, such as the existence of significant gel-to-gel variability, sensitivity and the possibility of comigration of

391 several proteins in one single spot [38, 39]. 2D-DIGE was implemented as a
392 quantitative alternative to conventional 2D electrophoresis [40, 41]. Whilst most of the
393 drawbacks of classic 2D were overcome, spot comigration remains an unsolved issue.
394 Moreover, a bias toward high-abundant proteins may have been introduced by the use
395 of Coomasie staining preparative gels. Alternative approaches for future work such as
396 gel-free quantitative MS proteomics (i.e. iTRAQ labeling, label-free methods) would
397 overcome these limitations [42]. In addition, our study deals with the relatively mild
398 effects on proteomic and gene-expression patterns [43] characteristic of dietary
399 interventions in nutrition research. Therefore, the protein spots that were considered in
400 the analysis were the ones that reached a theoretical optimal fold-cutoff of 1.18 and
401 were statistically significant using. Despite these limitations, eighteen proteins were
402 identified as squalene targets in apoE-ko mice. Twelve of them were significantly
403 associated with hepatic fat content, and among them, MAT1A and ACADS, showed
404 changes at the mRNA level consistent with the changes in protein abundance.
405 The initial step in fatty acid β-oxidation is catalyzed by a family of acyl-CoA
406 dehydrogenases including ACADS whose function is exerted on short-chain acyl-CoA
407 [5]. ACADS spot levels were significantly decreased in squalene fed apoE ko mice.
408 Furthermore, these levels were correlated with hepatic fat content which reinforces its
409 putative involvement in triglyceride metabolism control. Furthermore, squalene-
410 induced decrease in ACADS expression was already at the mRNA level in apoE-ko
411 mice. In addition, these mice displayed an increased expression of this mRNA
412 compared to wild-type that correlates with the appearance of fatty liver. Thus, ACADS
413 seems a marker of hepatic steatosis and may play a role in this condition's amelioration
414 induced by squalene, what is in agreement with a genome-wide association study

finding that some variants of this gene were associated with impaired fatty acid beta-oxidation [44].

Even though we did not find any modification in protein levels of the mitochondrial oxidative phosphorylation system components, we thought it interesting to test for its biogenesis and activity being the integrating point of mitochondrial metabolism, mainly for ATP synthesis. Squalene feeding did not show any apparent effect on the mitochondrial respiratory chain complex assembly levels as observed in the Blue-Native/Western Blot and In-Gel activity assays, although these are not quantitative measurements. The oxygen consumption rate was the same in liver mitochondria isolated from treated and untreated animals, suggesting that albeit fatty acid *β*-oxidation is altered by introducing squalene in the diet, the endpoint of the electron flow generated by it is unchanged. However, we did observe an increase in the maximum cytochrome c oxidase activity (COX or Complex IV). It is beyond the scope of this report to go deeper in the analysis of this effect, but one could argue that increased squalene dietary levels are triggering a response in which COX activity is increased, by means of phosphorylation of specific residues, in order to switch from an "energy storage" mode to an "energy consuming" mode, as suggested in a recent report [45]. This enhancement in COX activity was not followed by increased total oxygen consumption, probably because in this situation the activity of the other rate-limiting mitochondrial respiratory components is not induced by squalene.

Another important finding of this study was the increased METK1 (MAT1A) expression in the squalene group, both at the protein and mRNA levels. It is interesting to note its presence in the mitochondrial fraction since it has always been considered a cytosolic and nuclear protein [46]. In addition, it is accompanied by another cytosolic protein involved in methionine metabolism: FAAA [47], but not by classical cytosolic

proteins such as lactate dehydrogenase or alanine aminotransferase (data not shown). If these findings are due either to selective contamination of proteins that are present in our fractions because they are physically associated with mitochondria, or to the fact that they are indeed inside the organelle remain to be established. Methionine adenosyltransferases are the products of two genes, *MAT1A* and *MAT2A*, which catalyze the formation of *S*-adenosyl-L-methionine (SAMe), the principal biological methyl donor. In mammals, up to 85% of all methylation reactions and up to 48% of methionine metabolism occurs in the liver, which indicates the important role of this organ in the regulation of blood methionine. Apart from its role in methionine catabolism, SAMe also is an intracellular key regulator of liver essential functions for its regeneration and differentiation, as well as hepatocyte sensitivity to apoptosis and cell death [48, 49]. MAT1A is the isoform present in adult liver, and mice lacking the *Mat1a* gene exhibited a chronic reduction in hepatic SAMe levels and spontaneous development of nonalcoholic steatohepatitis [50] and hepatocellular carcinoma [51] mediated by complex signalling pathways [52-54]. Recently, *Mat1a* deficiency has been associated with NAFLD being its function controlling phosphatidylcholine-mediated processing of sterol regulatory element binding protein 1 [55] required for very low density lipoprotein assembly and plasma lipid homeostasis in mice [56]. Furthermore, MAT1A variants in humans were strongly associated with hypertension and stroke independently of homocysteine levels [57]. On the other hand, *in vivo* overexpression of *Mat1a* in liver cancer cells suppressed tumor growth, being a putative strategy to treat hepatocellular carcinoma [58]. Therefore, the relevant role of MAT1A in VLDL metabolism [56] may explain its increased expression in squalene-treated mice and the significant correlation with hepatic fat content (Table 2). In our model, MAT1A levels were not associated with lipid droplet size (data not shown) suggesting it is not involved

in this process but more related to VLDL triglycerides assembly, as described in the literature[56]. However, we did not observe any change in plasma triglycerides [18], nor in APOA5 what might also indicate an activation of lipoprotein lipase in our setting. Deficiency in *Mat1a* was also found associated with increased oxidative stress [59]. On the other hand, increases in *Mat1a* expression associated with accumulation of SAMe, were translated in liver steatosis, fibrosis, and hepatic carcinoma in *Gnmt*-KO mice [60]. In another model, *Cbs*-KO mice, presenting low SAMe content [61] was found associated with increased levels of Mat1a (data not shown) and progression of hepatic steatosis [20]. SAMe is a coenzyme involved in more than three-hundred biochemical reactions, some of them compartmentalized in the nucleus (DNA methyltransferases), reticulum (phosphatidylethanolamine methyltrasnferase) or cytosol (glycine N-methyltransferase or guanidinoacetate N-methyltransferase), therefore, its levels vary extraordinarily in reflection of folate, methionine or nicotinamide nutritional status and of the specific requirements of a particular compartment or metabolic pathway [62]. Overall, considering MAT1 dual role in liver pathology, the interpretation of the observed increased expression in squalene-treated mice has to be made with caution, taken into account also other multiple markers of the hepatic energetic status and oxidative stress as for example, prostanoids [63],[6]. Interestingly, an important decrease in serum 8-isoprostaglandin$F_{2\alpha}$ was observed in mice receiving squalene [18] reflecting less oxidative stress, in agreement with previous reports [64]. Furthermore, our results showing that squalene administration produces an up-regulation of stearoyl-CoA desaturase (*Scd1*), which increases monounsaturated fatty acid and safe lipid stores [65] could contribute to the squalene protective effect. In this sense, increases in *Ppara and Cyp7a1*, involved in fatty acid and cholesterol catabolic pathways [6] might indicate an increased catabolism of these compounds for the liver to get rid of fatty acids and

cholesterol. These findings open interesting possibilities regarding the possible effects of squalene in more advanced liver diseases, which would be particularly attractive considering its low toxicity.

Taken together, proteomic experiments point out the implication of squalene in carbohydrate, amino acid and lipid metabolism resulting in amelioration of steatotic liver in apoE knockout mice. In particular, our data show a clear modulation of enzymes implicated in β-oxidation. Protein changes were concordant with the observed RNA levels for *Mat1a* and *Acads.* The former mRNA increases after receiving squalene, in both apoE knock-out and wild-type mice, together with those of *Scd1, Ppara, and Cyp7a1*, which, although never described before as such, are most probably also squalene targets. The variation in *Acads* expression was more pronounced when fatty liver was present and was associated with the beneficial effect of squalene, suggesting a novel role for this protein in steatosis development.

Acknowledgments

This research was supported by grants from CIBER Fisiopatología de la Obesidad y Nutrición as an initiative of FEDER- ISCIII, FEDER-CICYT (SAF 2010-14958), *Redes* DGA (B-69) and Gobierno de Aragón (PI025/08). We thank Irene Orera from the Unidad de Proteómica of IIS and Aurora Gómez-Duran and Julio Montoya from CIBERER for their help in the experiments. A.R. was recipient of a DGA grant. No competing financial interests exist.

Abbreviations

Acaca, acetyl-Coenzyme A carboxylase alpha; *Acacb*, acetyl-Coenzyme A carboxylase beta; ACADS, short-chain specific acyl-CoA dehydrogenase; AL7A1, alpha-aminoadipic semialdehyde dehydrogenase; ALDH2, alpha-aminoadipic semialdehyde dehydrogenase; APOA1, apolipoprotein A1; ASSY, argininosuccinate synthase; CAH3, carbonic anhydrase 3; *Cyp7a1*, cytochrome P450, family 7, subfamily a, polypeptide 1; DHE3, glutamate dehydrogenase; DHSO, sorbitol dehydrogenase; ECHM, enoyl-CoA hidratase; ETFB, electron flavoprotein subunit beta; FAAA, fumarylacetoacetase; FA, fatty acid; HDL, high density lipoprotein; INMT, indolethylamine N-methyltransferase; KAD2, adenylate kinase 2; KAD4, adenylate kinase isoenzyme 4; LDL, low density lipoprotein; METK1 (MAT1A), sadenosylmethionine synthase isoform type1; MIQE, minimum information for publication of quantitative real time PCR experiments; PANTHER, protein analysis through evolutionary relationships; *Ppargc1a*, peroxisome proliferative activated receptor, gamma, coactivator 1 alpha; RGN, regucalcin; *Scd1*, stearoyl-Coenzyme A desaturase 1; THIM, 3-ketoacyl-CoA thiolase; ZADH2, zinc-binding alcohol dehydrogenase domain-containing protein 2.

References

[1] Kantartzis K, Schick F, Haring HU, Stefan N. Environmental and genetic determinants of fatty liver in humans. Dig Dis. 2010;28:169-78.

[2] Tiniakos DG, Vos MB, Brunt EM. Nonalcoholic fatty liver disease: pathology and pathogenesis. Annu Rev Pathol. 2010;5:145-71.

[3] Day CP. Genetic and environmental susceptibility to non-alcoholic fatty liver disease. Dig Dis. 2010;28:255-60.

[4] Bass NM. Lipidomic dissection of nonalcoholic steatohepatitis: moving beyond foie gras to fat traffic. Hepatology. 2010;51:4-7.

[5] Musso G, Gambino R, Cassader M. Recent insights into hepatic lipid metabolism in non-alcoholic fatty liver disease (NAFLD). Prog Lipid Res. 2009;48:1-26.

[6] Lou-Bonafonte JM, Arnal C, Osada J. New genes involved in hepatic steatosis. Curr Opin Lipidol. 2011;22:159-64.

[7] Acin S, Navarro MA, Perona JS, Surra JC, Guillen N, Arnal C, et al. Microarray analysis of hepatic genes differentially expressed in the presence of the unsaponifiable fraction of olive oil in apolipoprotein E-deficient mice. Br J Nutr. 2007;97:628-38.

[8] Assy N, Nassar F, Nasser G, Grosovski M. Olive oil consumption and non-alcoholic fatty liver disease. World J Gastroenterol. 2009;15:1809-15.

[9] Arbones-Mainar JM, Ross K, Rucklidge GJ, Reid M, Duncan G, Arthur JR, et al. Extra virgin olive oils increase hepatic fat accumulation and hepatic antioxidant protein levels in APOE-/- mice. J Proteome Res. 2007;6:4041-54.

[10] María-Isabel Covas DPharm VR-GRdlTD, Anthony Kafatos MD, Rosa M. Lamuela-Raventós DPharm, Jesus Osada DPharm, Robert W. Owen BSc, Francesco Visioli. Minor Components of Olive Oil: Evidence to Date of Health Benefits in Humans. Nutrition Reviews. 2006;64:s20-s30.

[11] Perona JS, Cabello-Moruno R, Ruiz-Gutierrez V. The role of virgin olive oil components in the modulation of endothelial function. J Nutr Biochem. 2006;17:429-45.

559 [12] Konstantinidou V, Covas MI, Munoz-Aguayo D, Khymenets O, de la Torre R,
560 Saez G, et al. In vivo nutrigenomic effects of virgin olive oil polyphenols within
561 the frame of the Mediterranean diet: a randomized controlled trial. FASEB J.
562 2010;24:2546-57.

563 [13] Owen RW, Mier W, Giacosa A, Hull WE, Spiegelhalder B, Bartsch H. Phenolic
564 compounds and squalene in olive oils: the concentration and antioxidant potential
565 of total phenols, simple phenols, secoiridoids, lignansand squalene. Food Chem
566 Toxicol. 2000;38:647-59.

567 [14] Murkovic M, Lechner S, Pietzka A, Bratacos M, Katzogiannos E. Analysis of
568 minor components in olive oil. J Biochem Biophys Methods. 2004;61:155-60.

569 [15] Smith TJ. Squalene: potential chemopreventive agent. Expert Opin Investig
570 Drugs. 2000;9:1841-8.

571 [16] Gylling H, Miettinen TA. Postabsorptive metabolism of dietary squalene.
572 Atherosclerosis. 1994;106:169-78.

573 [17] Aguilera Y, Dorado ME, Prada FA, Martinez JJ, Quesada A, Ruiz-Gutierrez V.
574 The protective role of squalene in alcohol damage in the chick embryo retina. Exp
575 Eye Res. 2005;80:535-43.

576 [18] Guillen N, Acin S, Navarro MA, Perona JS, Arbones-Mainar JM, Arnal C, et al.
577 Squalene in a sex-dependent manner modulates atherosclerotic lesion which
578 correlates with hepatic fat content in apoE-knockout male mice. Atherosclerosis.
579 2008;197:72-83.

580 [19] Sarria AJ, Surra JC, Acin S, Carnicer R, Navarro MA, Arbones-Mainar JM, et al.
581 Understanding the role of dietary components on atherosclerosis using genetic
582 engineered mouse models. Front Biosci. 2006;11:955-67.

583 [20] Guillen N, Navarro MA, Arnal C, Noone E, Arbones-Mainar JM, Acin S, et al.
584 Microarray analysis of hepatic gene expression identifies new genes involved in
585 steatotic liver. Physiol Genomics. 2009;37:187-98.

586 [21] Arbones-Mainar JM, Navarro MA, Guzman MA, Arnal C, Surra JC, Acin S, et al.
587 Selective effect of conjugated linoleic acid isomers on atherosclerotic lesion
588 development in apolipoprotein E knockout mice. Atherosclerosis. 2006;189:318-
589 27.

590 [22] Arbones-Mainar JM, Navarro MA, Acin S, Guzman MA, Arnal C, Surra JC, et al.
591 Trans-10, cis-12- and cis-9, trans-11-conjugated linoleic acid isomers selectively
592 modify HDL-apolipoprotein composition in apolipoprotein E knockout mice. J
593 Nutr. 2006;136:353-9.

594 [23] Fromenty B, Robin MA, Igoudjil A, Mansouri A, Pessayre D. The ins and outs of
595 mitochondrial dysfunction in NASH. Diabetes Metab. 2004;30:121-38.

596 [24] Bonomini F, Filippini F, Hayek T, Aviram M, Keidar S, Rodella LF, et al.
597 Apolipoprotein E and its role in aging and survival. Exp Gerontol. 2009;45:149-
598 57.

599 [25] Nakamura T, Watanabe A, Fujino T, Hosono T, Michikawa M. Apolipoprotein E4
600 (1-272) fragment is associated with mitochondrial proteins and affects
601 mitochondrial function in neuronal cells. Mol Neurodegener. 2009;4:35.

602 [26] Suski M, Olszanecki R, Madej J, Toton-Zuranska J, Niepsuj A, Jawien J, et al.
603 Proteomic analysis of changes in protein expression in liver mitochondria in apoE
604 knockout mice. J Proteomics. 2011;74:887-93.

605 [27] Enriquez JA, Perez-Martos A, Fernandez-Silva P, Lopez-Perez MJ, Montoya J.
606 Specific increase of a mitochondrial RNA transcript in chronic ethanol-fed rats.
607 FEBS Lett. 1992;304:285-8.

608 [28] Fernandez-Vizarra E, Ferrin G, Perez-Martos A, Fernandez-Silva P, Zeviani M,
609 Enriquez JA. Isolation of mitochondria for biogenetical studies: An update.
610 Mitochondrion. 2009;10:253-62.

611 [29] Kirby DM, Thorburn DR, Turnbull DM, Taylor RW. Biochemical assays of
612 respiratory chain complex activity. Methods Cell Biol. 2007;80:93-119.

613 [30] Schagger H. Native electrophoresis for isolation of mitochondrial oxidative
614 phosphorylation protein complexes. Methods Enzymol. 1995;260:190-202.

615 [31] Calvaruso MA, Smeitink J, Nijtmans L. Electrophoresis techniques to investigate
616 defects in oxidative phosphorylation. Methods. 2008;46:281-7.

617 [32] Barcelo-Batllori S, Kalko SG, Esteban Y, Moreno S, Carmona MC, Gomis R.
618 Integration of DIGE and bioinformatics analyses reveals a role of the antiobesity
619 agent tungstate in redox and energy homeostasis pathways in brown adipose
620 tissue. Mol Cell Proteomics. 2008;7:378-93.

621 [33] Bustin SA. Why the need for qPCR publication guidelines?--The case for MIQE.
622 Methods. 2009/12/23 ed2010. p. 217-26.

623 [34] Livak KJ, Schmittgen TD. Analysis of relative gene expression data using real-
624 time quantitative PCR and the 2(-Delta Delta C(T)) Method. Methods.
625 2001;25:402-8.

626 [35] Mi H, Dong Q, Muruganujan A, Gaudet P, Lewis S, Thomas PD. PANTHER
627 version 7: improved phylogenetic trees, orthologs and collaboration with the Gene
628 Ontology Consortium. Nucleic Acids Res. 2009;38:D204-10.

629 [36] Gygi SP, Rochon Y, Franza BR, Aebersold R. Correlation between protein and
630 mRNA abundance in yeast. Mol Cell Biol. 1999;19:1720-30.

631 [37] Aebersold R, Mann M. Mass spectrometry-based proteomics. Nature.
632 2003;422:198-207.

633 [38] Campostrini N, Areces LB, Rappsilber J, Pietrogrande MC, Dondi F, Pastorino F,
634 et al. Spot overlapping in two-dimensional maps: a serious problem ignored for
635 much too long. Proteomics. 2005;5:2385-95.

636 [39] Corthals GL, Wasinger VC, Hochstrasser DF, Sanchez JC. The dynamic range of
637 protein expression: a challenge for proteomic research. Electrophoresis.
638 2000;21:1104-15.

639 [40] Unlu M, Morgan ME, Minden JS. Difference gel electrophoresis: a single gel
640 method for detecting changes in protein extracts. Electrophoresis. 1997;18:2071-
641 7.

642 [41] Marouga R, David S, Hawkins E. The development of the DIGE system: 2D
643 fluorescence difference gel analysis technology. Anal Bioanal Chem.
644 2005;382:669-78.

645 [42] Gartner CA, Elias JE, Bakalarski CE, Gygi SP. Catch-and-release reagents for
646 broadscale quantitative proteomics analyses. J Proteome Res. 2007;6:1482-91.

647 [43] Afman L, Muller M. Nutrigenomics: from molecular nutrition to prevention of
648 disease. J Am Diet Assoc. 2006;106:569-76.

649 [44] Illig T, Gieger C, Zhai G, Romisch-Margl W, Wang-Sattler R, Prehn C, et al. A
650 genome-wide perspective of genetic variation in human metabolism. Nat Genet.
651 2010;42:137-41.

652 [45] Acin-Perez R, Gatti DL, Bai Y, Manfredi G. Protein phosphorylation and
653 prevention of cytochrome oxidase inhibition by ATP: coupled mechanisms of
654 energy metabolism regulation. Cell Metab. 2011;13:712-9.

655 [46] Reytor E, Perez-Miguelsanz J, Alvarez L, Perez-Sala D, Pajares MA.
656 Conformational signals in the C-terminal domain of methionine
657 adenosyltransferase I/III determine its nucleocytoplasmic distribution. FASEB J.
658 2009;23:3347-60.

659 [47] Mudd SH. Hypermethioninemias of genetic and non-genetic origin: A review. Am
660 J Med Genet C Semin Med Genet. 2011;157:3-32.

661 [48] Corrales FJ, Perez-Mato I, Sanchez Del Pino MM, Ruiz F, Castro C, Garcia-
662 Trevijano ER, et al. Regulation of mammalian liver methionine
663 adenosyltransferase. J Nutr. 2002;132:2377S-81S.

664 [49] Mato JM, Corrales FJ, Lu SC, Avila MA. S-Adenosylmethionine: a control switch
665 that regulates liver function. FASEB J. 2002;16:15-26.

666 [50] Lu SC, Alvarez L, Huang ZZ, Chen L, An W, Corrales FJ, et al. Methionine
667 adenosyltransferase 1A knockout mice are predisposed to liver injury and exhibit
668 increased expression of genes involved in proliferation. Proc Natl Acad Sci U S
669 A. 2001;98:5560-5.

670 [51] Martinez-Chantar ML, Corrales FJ, Martinez-Cruz LA, Garcia-Trevijano ER,
671 Huang ZZ, Chen L, et al. Spontaneous oxidative stress and liver tumors in mice
672 lacking methionine adenosyltransferase 1A. FASEB J. 2002;16:1292-4.

673 [52] Martinez-Lopez N, Varela-Rey M, Fernandez-Ramos D, Woodhoo A, Vazquez-
674 Chantada M, Embade N, et al. Activation of LKB1-Akt pathway independent of
675 phosphoinositide 3-kinase plays a critical role in the proliferation of
676 hepatocellular carcinoma from nonalcoholic steatohepatitis. Hepatology.
677 2010;52:1621-31.

678 [53] Santamaria E, Avila MA, Latasa MU, Rubio A, Martin-Duce A, Lu SC, et al.
679 Functional proteomics of nonalcoholic steatohepatitis: mitochondrial proteins as
680 targets of S-adenosylmethionine. Proc Natl Acad Sci U S A. 2003;100:3065-70.

681 [54] Tomasi ML, Ramani K, Lopitz-Otsoa F, Rodriguez MS, Li TW, Ko K, et al. S-
682 adenosylmethionine regulates dual-specificity mitogen-activated protein kinase
683 phosphatase expression in mouse and human hepatocytes. Hepatology.
684 2010;51:2152-61.

685 [55] Walker AK, Jacobs RL, Watts JL, Rottiers V, Jiang K, Finnegan DM, et al. A
686 Conserved SREBP-1/Phosphatidylcholine Feedback Circuit Regulates
687 Lipogenesis in Metazoans. Cell. 2011;147:840-52.

688 [56] Cano A, Buque X, Martinez-Una M, Aurrekoetxea I, Menor A, Garcia-Rodriguez
689 JL, et al. Methionine adenosyltransferase 1A gene deletion disrupts hepatic VLDL
690 assembly in mice. Hepatology. 2011;54:1975-86.

691 [57] Lai CQ, Parnell LD, Troen AM, Shen J, Caouette H, Warodomwichit D, et al.
692 MAT1A variants are associated with hypertension, stroke, and markers of DNA
693 damage and are modulated by plasma vitamin B-6 and folate. Am J Clin Nutr.
694 2010;91:1377-86.

695 [58] Li J, Ramani K, Sun Z, Zee C, Grant EG, Yang H, et al. Forced expression of
696 methionine adenosyltransferase 1A in human hepatoma cells suppresses in vivo
697 tumorigenicity in mice. Am J Pathol. 2010;176:2456-66.

698 [59] Rubio A, Guruceaga E, Vazquez-Chantada M, Sandoval J, Martinez-Cruz LA,
699 Segura V, et al. Identification of a gene-pathway associated with non-alcoholic
700 steatohepatitis. J Hepatol. 2007;46:708-18.

701 [60] Martinez-Chantar ML, Vazquez-Chantada M, Ariz U, Martinez N, Varela M, Luka
702 Z, et al. Loss of the glycine N-methyltransferase gene leads to steatosis and
703 hepatocellular carcinoma in mice. Hepatology. 2008;47:1191-9.

704 [61] Dayal S, Bottiglieri T, Arning E, Maeda N, Malinow MR, Sigmund CD, et al.
705 Endothelial dysfunction and elevation of S-adenosylhomocysteine in
706 cystathionine beta-synthase-deficient mice. Circ Res. 2001;88:1203-9.

[62] Varela-Rey M, Martinez-Lopez N, Fernandez-Ramos D, Embade N, Calvisi DF, Woodhoo A, et al. Fatty liver and fibrosis in glycine N-methyltransferase knockout mice is prevented by nicotinamide. Hepatology. 2010;52:105-14.

[63] Barr J, Vazquez-Chantada M, Alonso C, Perez-Cormenzana M, Mayo R, Galan A, et al. Liquid chromatography-mass spectrometry-based parallel metabolic profiling of human and mouse model serum reveals putative biomarkers associated with the progression of nonalcoholic fatty liver disease. J Proteome Res. 2010;9:4501-12.

[64] Buddhan S, Sivakumar R, Dhandapani N, Ganesan B, Anandan R. Protective effect of dietary squalene supplementation on mitochondrial function in liver of aged rats. Prostaglandins Leukot Essent Fatty Acids. 2007;76:349-55.

[65] Li ZZ, Berk M, McIntyre TM, Feldstein AE. Hepatic lipid partitioning and liver damage in nonalcoholic fatty liver disease: role of stearoyl-CoA desaturase. J Biol Chem. 2009;284:5637-44.

722 **Fig. 1. Analyses of lipid droplet size in apoE-ko mice**. A) Average lipid droplet
723 diameter in experimental groups (control and squalene, n=5, respectively). B) Droplet
724 size distribution into 5 categories in control and squalene-treated mice groups.
725 Diameters of 100 droplets per mouse of both experimental groups were measured and
726 expressed in □m. Mann–Whitney *U*-test was used for the statistical analyses. **P <
727 0.01 and *P < 0.05.

728 **Fig. 2. Mitochondrial characterization.** A) COX and CS enzymatic activities of
729 control and squalene-treated animals were measured in mitochondria isolated from two
730 liver wild-type tissue pools, from three animals each. B) From top to bottom, complex I
731 in-gel activity (CI-IGA) and Western blot analyses of the different mitochondrial
732 respiratory chain enzymes (Complexes I, II, III and IV). Mann–Whitney *U*-test was
733 used in the statistical analyses. *P < 0.05.

734 **Fig. 3. Proteome analyses of mitochondrial fractions.** A) Representative images of
735 Cy2, Cy3, Cy5 and the overlap of the 3 dyes of 2-DE gels from apoE-ko mice. B) 2D
736 preparative Coomassie-stained gel with 19 spots exhibiting statistically significant
737 differences. Spot numbers correspond to proteins shown in Table 1. C) Spot pairs
738 corresponding to up-regulated ASSY, METK1 and down-regulated ACADS and
739 ALDH2.

740 **Fig. 4. Gene ontology groupings using the PANTHER classification system**
741 (www.pantherdb.org). Classification of the identified changed proteins according to A)
742 biological processes and B) molecular functions.

743 **Fig. 5. Effect of squalene on hepatic *Mat1a* and *Acads* mRNA levels.** A) Hepatic
744 mRNA levels were measured in apoE-ko (n=5, for each group) and wild-type (n=7, for
745 each group) mice. Results are expressed as mean±SEM of arbitrary absorbance units

normalized to the *Cyclophilin B* gene expression with the qPCR analysis. Mann–Whitney *U*-test was used for the statistical analyses. **P < 0.01; *P < 0.05. B) Correlation analysis among liver fat content and hepatic mRNA levels in apoE-deficient mice.

Fig. 6. Correlation analysis among liver fat content and hepatic mRNA levels in apoE-deficient mice.

Table 1. List of spots and proteins differentially expressed between squalene-treated and control animals in apoE-deficient mice.

Spot number[a]	Fold change [b]	Protein name	UniProt ID	UniProt entry name	Gene symbol	Mascot score[c]	Sequence coverage (%)	Peptides[d]	Ion score[e]	MW (kDa)[f]	pI[g]
1	1.99	Argininosuccinate synthase	P16460	ASSY	*Ass1*	357	45	20	238	46.6/44.2	8.36/9.14
2	1.40	Sadenosylmethionine synthase isoform type1	Q91X83	METK1	*Mat1a*	63	20	6	0	43.5/57.3	5.5/5.33
3	1.33	3-ketoacyl-CoA thiolase	Q8BWT1	THIM	*Acaa2*	170	35	13	89	41.9/43.2	8.33/9.36
4	–1.48	Alpha-aminoadipic semialdehyde dehydrogenase	Q9DBF1	AL7A1	*Aldh7a1*	391	45	33	225	58.9/68.7	7.16/5.99
5	–1.47	Alpha-aminoadipic semialdehyde dehydrogenase	P47738	ALDH2	*Aldh2*	159	7	6	137	56.5/63.5	7.5/6.28
6	–1.42	Indolethylamine N-methyltransferase	P40936	INMT	*Inmt*	115	23	7	78	29.5/28.7	6.0/5.75
7	–1.40	Glutamate dehydrogenase	P26443	DHE3	*Glud1*	1510	60	55	1193	61.3/64.2	8.0/7.30
8-10	–1.39	Carbonic anhydrase 3	P16015	CAH3	*Car3*	236	25	10	184	29.4/28.5	6.89/7.31
11	–1.38	Adenylate kinase 2	Q9WTP6	KAD2	*Ak2*	61	27	7	26	26.4/28.5	6.96/7.31
12,13	–1.35	Apolipoprotein A-I	Q00623	APOA1	*Apoa1*	87	17	6	57	30.58/25	5.64/5.24
14	–1.34	Adenylate kinase isoenzyme 4	Q9WUR9	KAD4	*Ak4*	100	62	14	17	25.1/35.0	7.02/6.80
15	–1.33	Regucalcin	Q64374	RGN	*Rgn*	277	51	16	152	33.4/36.7	5.16/4.54
16	–1.31	Fumarylacetoacetase	P35505	FAAA	*Fah*	61	17	8	25	46.1/41.5	6.92/7.36
17	–1.28	Electron flavoprotein subunit beta	Q9DCW4	ETFB	*Etfb*	97	59	18	0	27.6/28.1	8.25/8.09
18	–1.28	Enoyl-CoA hidratase	Q8BH95	ECHM	*Echs1*	161	31	10	96	31.4/30.1	8.76/8.47
19	–1.18	Sorbitol dehydrogenase	Q64442	DHSO	*Sord*	872	73	41	591	38.2/40.0	6.56/6.67
		Zinc-binding alcohol dehydrogenase domain-containing protein 2	Q8BGC4	ZADH2	*Zadh2*	146	44	17	71	40.5/40.5	7.01/6.67
		Short-chain specific acyl-CoA dehydrogenase	Q07417	ACADS	*Acads*	93	36	13	42	44.9/40.7	8.96/6.67

a. Spot numbers correspond to Figure 3

b. Positive and negative fold change in spot expression indicates up- and down-regulation of protein spots between squalene-treated between squalene-treated (n=5) and control (n=5) animals.

c. Mascot score: Protein Mascot Score based on MS and MSMS data (Protein Summary report). Protein scores > 61 were significant

(p<0.05)

d. **Number of matching peptides**
e. **Ion score: Mascot score which results from adding up individual MS/MS scores (Peptide Summary Report). Ion scores > 28 were significant (p<0.05)**
f. **Theoretical/calculated molecular weight of the matching protein**
g. **Theoretical/calculated isoelectric point of the matching protein**

753

Table 2. Correlation analysis among liver fat content and % normalized spot volume of control and squalene-treated apoE-deficient mice.

Gene	Coefficient correlation
ASSY	–0.794*
THIM	–0.721*
METK1	–0.661*
FAAA	0.891*
AL7A1	0.782*
INMT	0.758*
ACADS/ DHSO/ ZADH2	0.721*
CAH3	0.697*
DHE3	0.697*
KAD2	0.697*

754 Correlation study was done according to Spearman's test. *, $P < 0.05$.

Table 3. Hepatic mRNA expression of genes related to fatty acid and cholesterol metabolism following squalene administration

ApoE-ko mice	Control group (n=5)	Squalene group (n=5)
Acaca	1.2 ± 0.1	1.4 ± 0.2
Acacb	1.0 ± 0.2	1.6 ± 0.3
Scd1	0.7 ± 0.2	3.1 ± 0.5*
Cpt1a	0.9 ± 0.2	1.7 ± 0.4*
Ppara	1.1 ± 0.1	1.6 ± 0.2*
Ppargc1a	0.6 ± 0.1	5.4 ± 1.1**
Cyp7a1	0.9 ± 0.6	4.5 ± 0.5**
Wild-type mice	Control group (n=7)	Squalene group (n=7)
Acaca	1.2 ± 0.3	2.1 ± 0.4*
Acacb	1.1 ± 0.3	2.1 ± 0.2*
Scd1	1.2 ± 0.2	2.0 ± 0.2*
Cpt1a	1.1 ± 0.1	1.1 ± 0.2
Ppara	0.9 ± 0.1	1.6 ± 0.1*
Ppargc1a	0.8 ± 0.1	0.5 ± 0.1*
Cyp7a1	0.9 ± 0.2	1.6 ± 0.3*

Values are the means and SEM expressed as arbitrary units normalized to the cyclophilin B (*Ppib*) expression for each condition with the RT-qPCR analysis. Statistical analyses were done according to Mann–Whitney *U*-test. $^{**}P < 0.01$; $^{*}P < 0.05$.

Figure 1

Click here to download high resolution image

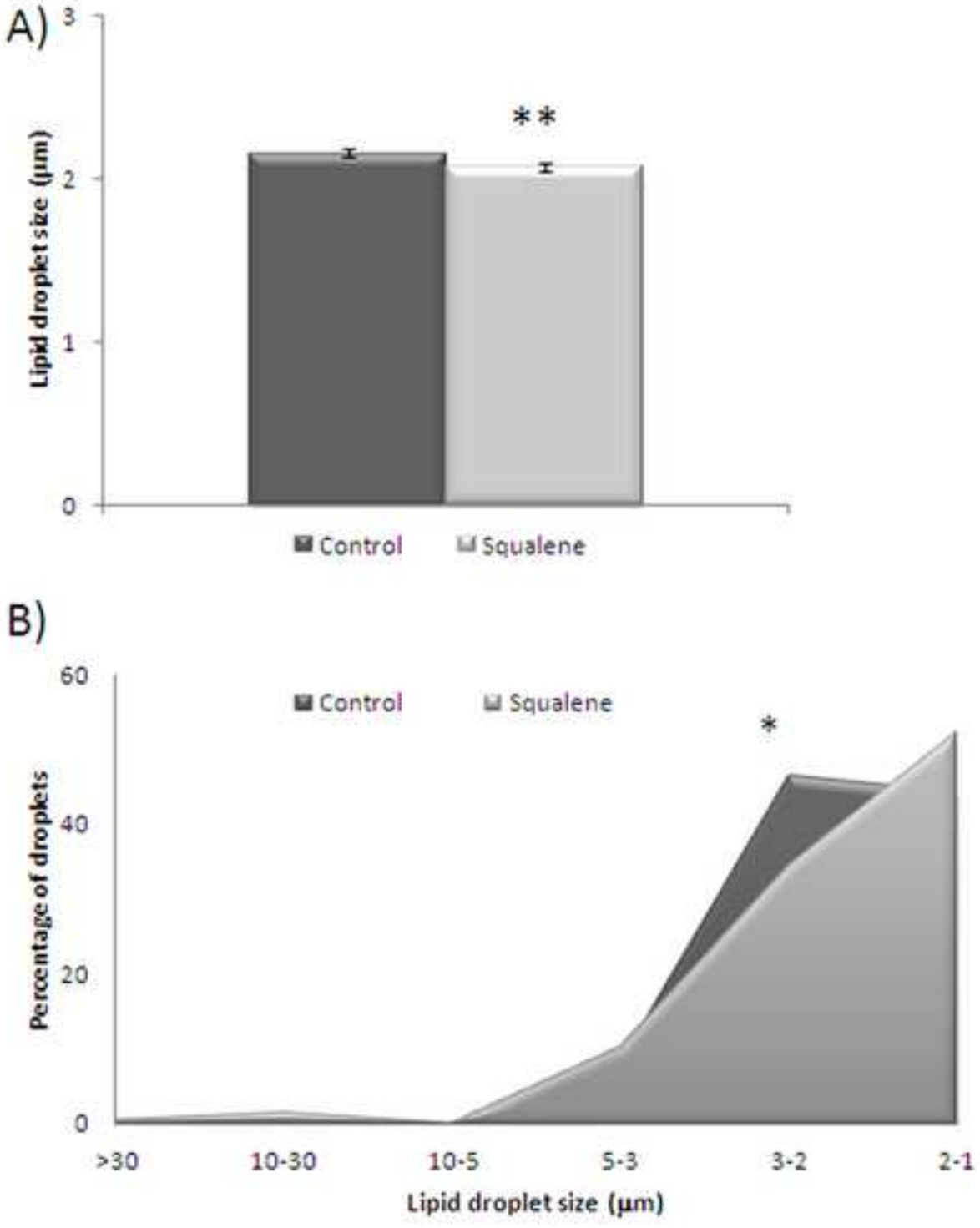

Figure 2

Click here to download high resolution image

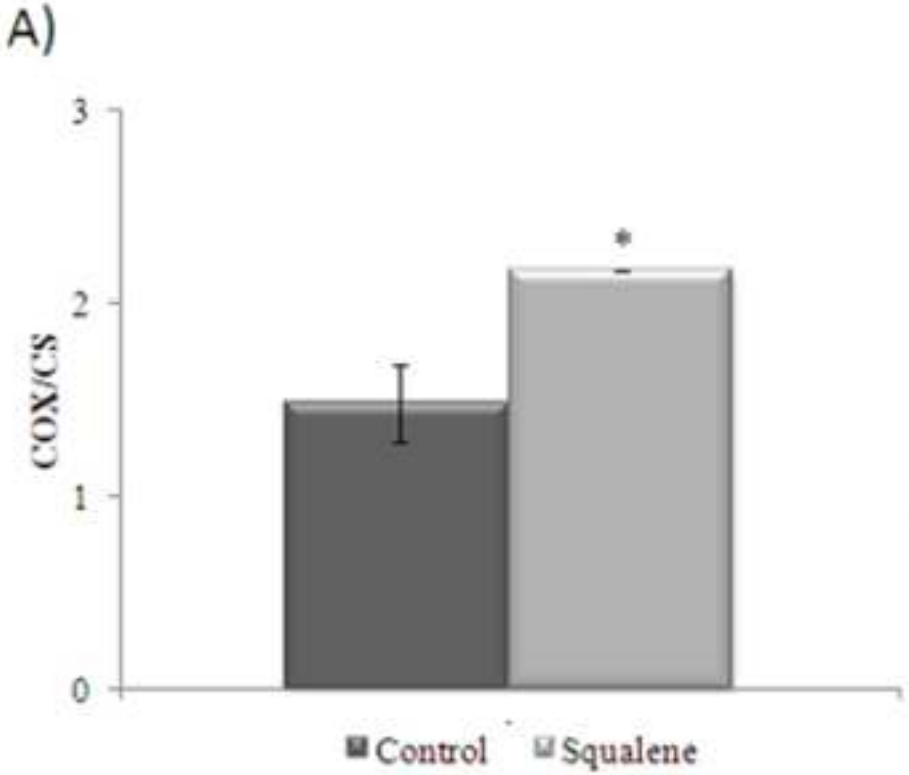

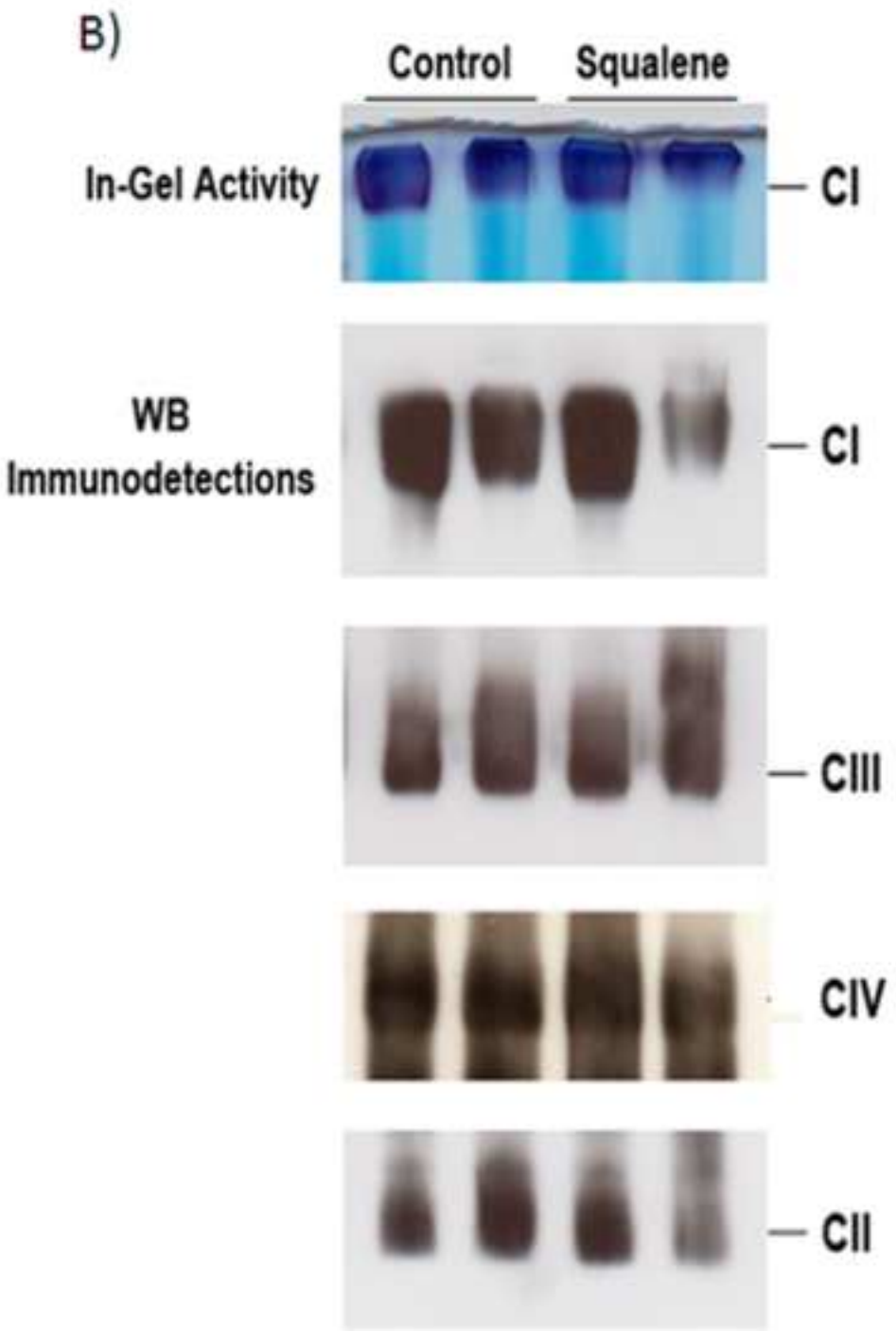

Figure 3

Click here to download high resolution image

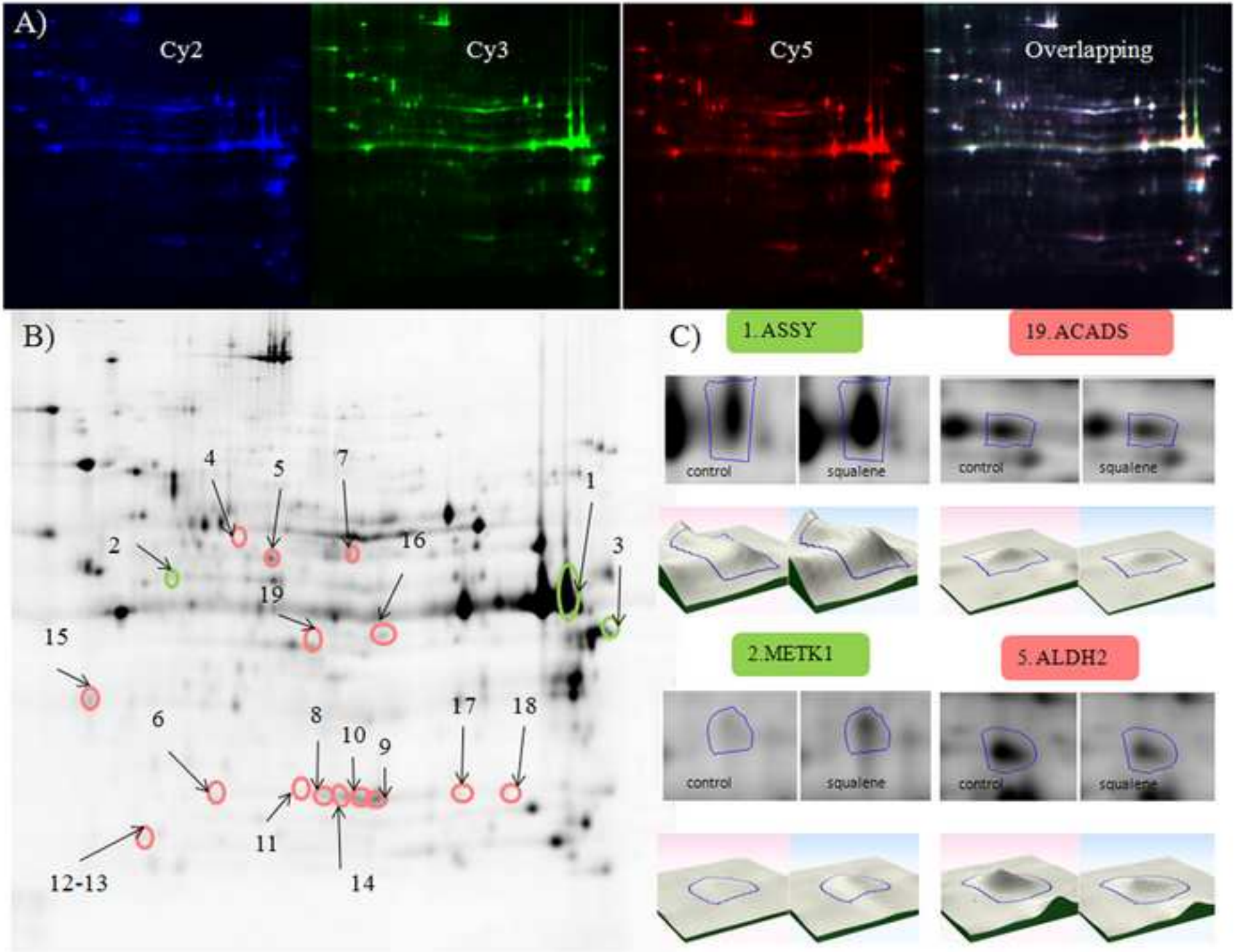

Figure 4

Click here to download high resolution image

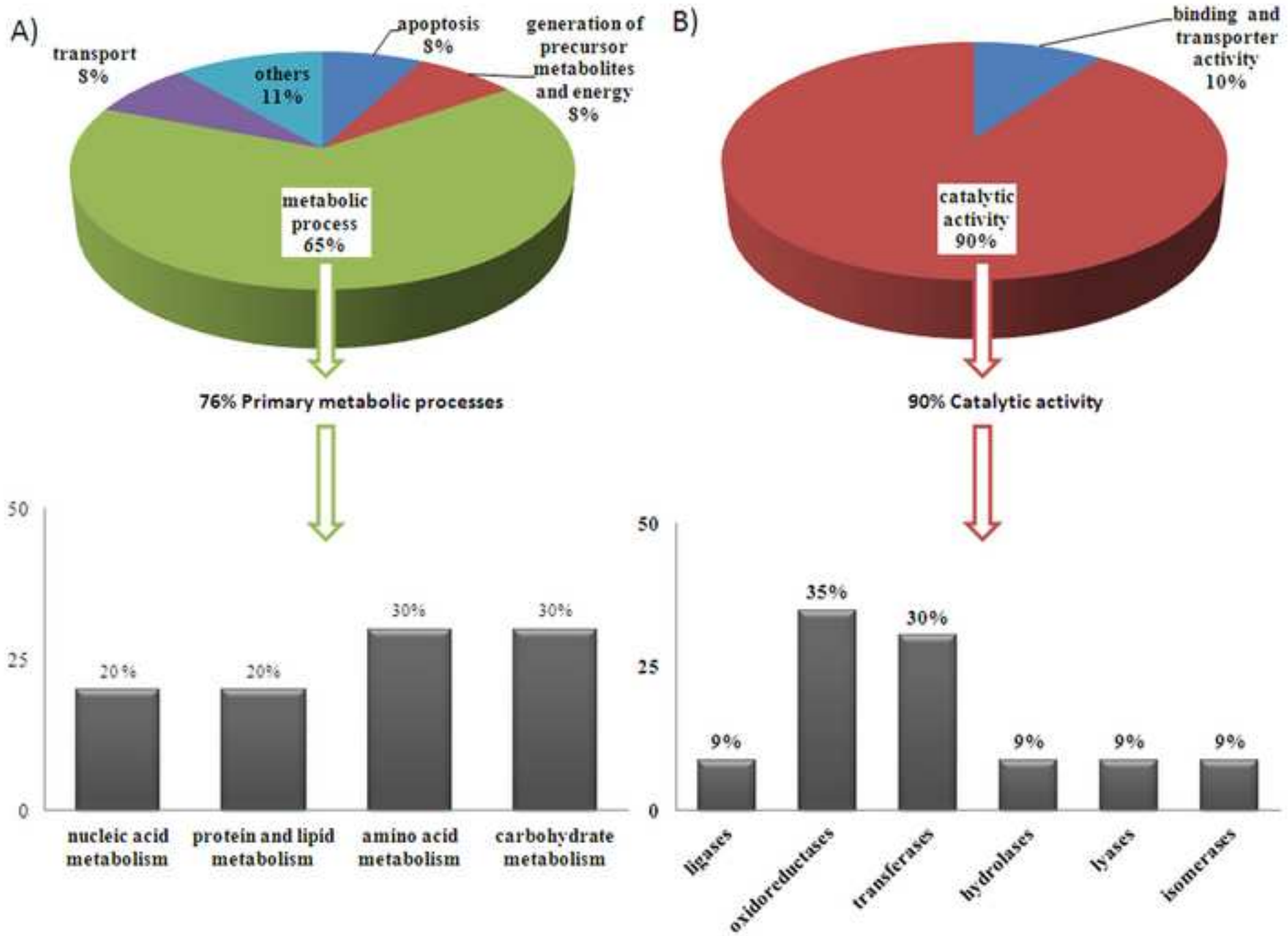

Figure 5

Click here to download high resolution image

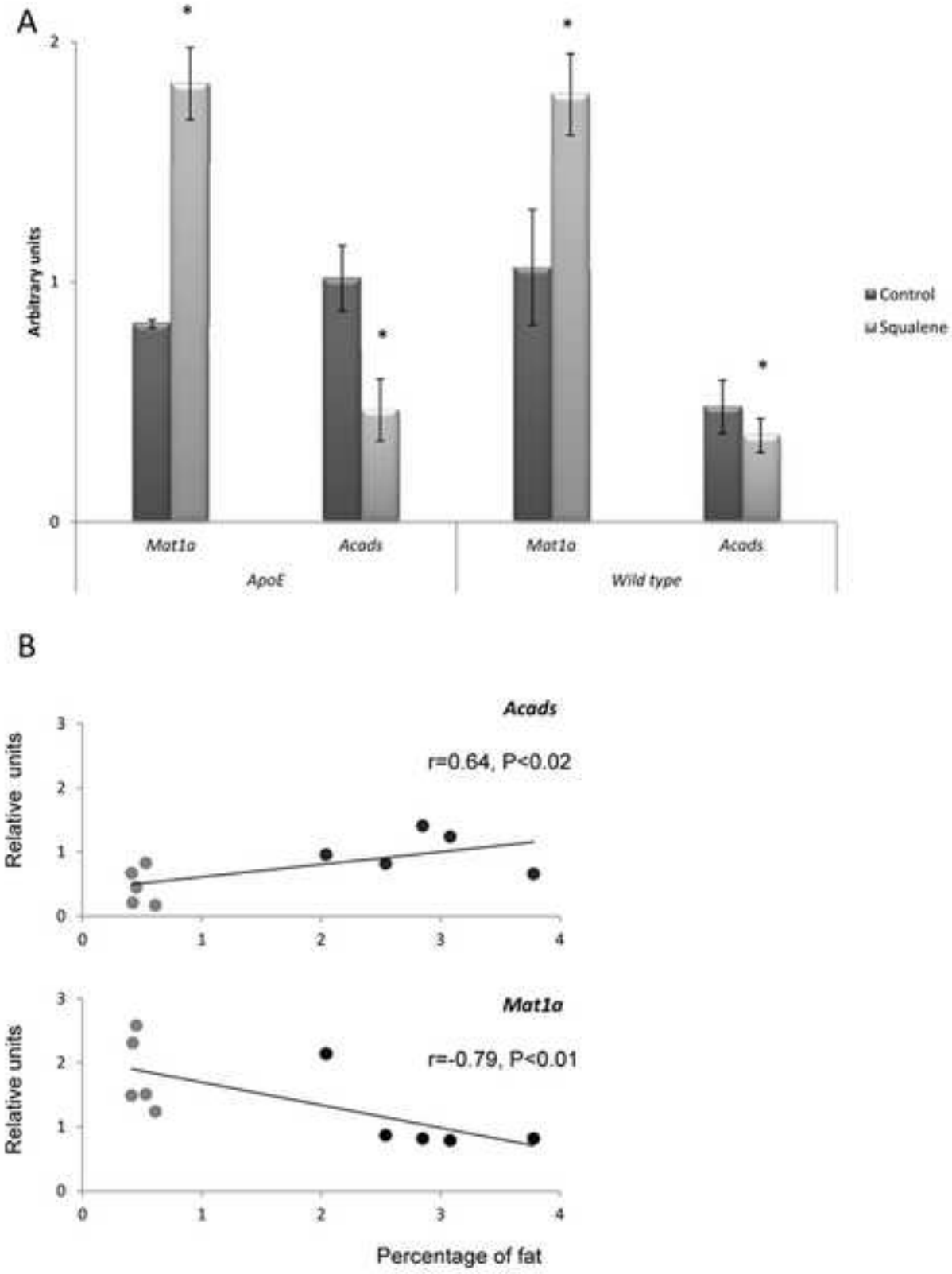

Figure 6

Click here to download high resolution image